

Determination of absolute photon yields under single-collision conditions

C. R. Dickson,^{a)} S. M. George,^{b)} and R. N. Zare^{c)}

Department of Chemistry, Columbia University, New York, New York 10027
(Received 27 December 1976)

The experimental procedure is presented to measure the absolute photon yield, the percentage probability of emitting a visible photon per reactant molecule consumed, for chemiluminescent reactions under single-collision conditions. Using a well-defined metal beam directed into a scattering gas at submillitorr pressures, this procedure is applied to the reactions $\text{Sm} + \text{N}_2\text{O}$, $\text{Sm} + \text{F}_2$, $\text{Ba} + \text{N}_2\text{O}$, and $\text{Ba} + \text{NO}_2$ to obtain the photon yields in the 350–800 nm range of 0.39%, 11.8%, 2.4%, and 0.18%, respectively, where the estimated uncertainty is about 50%. The absolute photon yields for each of these reactions initially increases with scattering gas pressure, demonstrating that secondary collisions “feed” radiating states from dark, reservoir states. It is suggested that other relative photon yields can be put on an absolute basis by comparison with the $\text{Sm} + \text{N}_2\text{O}$ chemiluminescent reaction.

I. INTRODUCTION

The possibility of a chemically pumped electronic-transition laser system has recently stimulated the measurement of absolute photon yields for several chemiluminescent reactions.^{1–6} Some of these reactions are reported to have high photon yields, such as $\text{Sm} + \text{F}_2$ (~60%),³ $\text{Sm} + \text{N}_2\text{O}$ (~35%),³ and $\text{Ba} + \text{N}_2\text{O}$ (~20%).^{3,6} All of these measurements were performed at pressures of several torr of argon and the fraction of electronic excitation appearing initially in the reaction products is obscured by the presence of many collisions. Thus, there is considerable interest in photon yield measurements in the submillitorr pressure range, because they provide information about the primary excitation process in a chemiluminescent reaction. We present here absolute photon yields for the reactions $\text{Sm} + \text{N}_2\text{O}$, $\text{Sm} + \text{F}_2$, $\text{Ba} + \text{N}_2\text{O}$, and $\text{Ba} + \text{NO}_2$ using a beam-gas arrangement at oxidant pressures of $\sim 10^{-4}$ torr.

Since absolute photon yields have not been determined in the submillitorr pressure range previously, our procedure will be presented in some detail. In particular, the following quantities are measured: the photon flux, the metal flux, the oxidant flux, and the chemiluminescent cross section and the total cross section for the reaction. The photon yield is defined to be the percentage number of photons emitted per oxidant molecule or metal atom consumed. For the beam-gas arrangement this is found from the ratio of the chemiluminescent cross section to the total reaction cross section.

We propose that the reaction of Sm with N_2O can be used as a reference reaction for beam-gas chemiluminescence for several reasons. This reaction appears to be bright under beam conditions as well as in the presence of argon. The spectrum of SmO resulting from this reaction (See Fig. 1) has little structure at low resolution ($\sim 5 \text{ \AA}$), and the chemiluminescence occurs over a wide

range of wavelengths (450–750 nm). Samarium is relatively cheap, undergoes far less oxidation in air than barium, and produces beams of high flux at temperatures easily achieved in most laboratories (1000–1200 °K). A well characterized reaction such as $\text{Sm} + \text{N}_2\text{O}$ now provides a basis for calibration in other laboratories as well as in our own.

II. EXPERIMENTAL

A. Beam apparatus

The beam apparatus LABSTAR, which has been described previously,⁷ is used to produce the chemiluminescent reactions. It consists of two differentially pumped chambers, the lower of which is a water-cooled Astro oven containing a cylindrical graphite heater and oven surrounded by three concentric tantalum heat shields (Fig. 2). The metal is heated until the vapor pressure reaches 0.01 to 0.1 torr. The effusive beam of metal enters the upper scattering chamber where it reacts with the oxidant molecules typically at pressures of 10^{-5} to 10^{-4} torr to produce chemiluminescence.

B. Photon flux

The approach often taken is to calibrate an entire optical-detection system (spectrometer, lens, etc.) on an absolute basis to determine the photon flux for a chemiluminescent reaction. This requires that one correct for the change in geometry when the standard lamp is

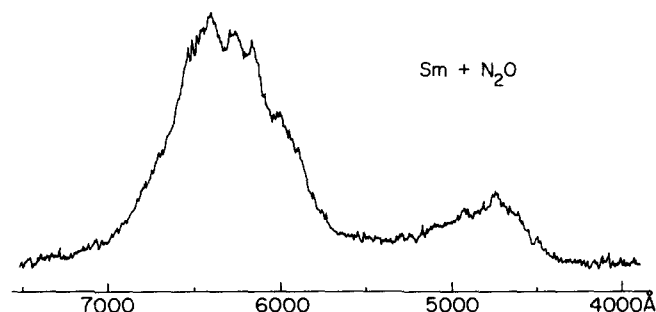


FIG. 1. Beam-gas chemiluminescent reaction of $\text{Sm} + \text{N}_2\text{O}$ taken at a scan rate of 500 Å/min and at a resolution of 5 Å.

^{a)}Present address: Materials Research Center, Allied Chemical, P. O. Box 1021R, Morristown, NJ 07960.

^{b)}Present address: Department of Chemistry, Yale University, New Haven, CT 06520.

^{c)}Present address: Department of Chemistry, Stanford University, Stanford, CA 94305.

TABLE I. Correction factors for chemiluminescent spectra.

$\lambda(\text{\AA})$	Standard lamp photon flux ^a	Relative photon flux ^b	Relative signal from optical-detection system ^c	Correction factor ^d
3000	0.00409	0.00124	0.001	1.000
3500	0.0288	0.00713	0.049	0.146
4000	0.0891	0.0221	0.202	0.109
4500	0.227	0.0562	0.475	0.118
5000	0.460	0.114	0.764	0.149
5500	0.773	0.191	0.973	0.196
6000	1.163	0.288	0.980	0.294
6500	1.601	0.396	0.881	0.449
7000	2.051	0.508	0.704	0.722
7500	2.515	0.623	0.445	1.400
8000	2.908	0.720	0.217	3.318
9000	3.557	0.880	0.016	55.
10000	4.040	1.000	0.008	125.

^aphotons sec⁻¹ cm⁻² nm⁻¹ × 10¹².^cSee Fig. 3(a).^bSee Fig. 3(c).^dSee Fig. 3(b).

placed at the position of the reaction zone. To avoid this difficulty, we have chosen to calibrate the optical-detection system that generates the spectra on a relative basis. We found that a relative calibration is reproducible to better than 1% under a variety of conditions (various spectrometer slit widths, with and without a lens in place, etc.). The results of the relative calibration of the optical-detection system used in our measurements are given in Table I. Figure 3 shows how the correction factors listed in Table I are generated. A scan of the standard lamp output is made with the spectrometer [Fig. 3(a)]. Figure 3(b) is a plot of the correction factors by which the standard lamp output [Fig. 3(a)] is multiplied to obtain the actual photon flux output of the standard lamp [Fig. 3(c)].

The spectrometer and optics (including the standard lamp) is aligned by means of a helium-neon laser. The common belief that uncalibrated lamps have the same absolute spectral output within 15% of that for a calibrated lamp is not correct. To obtain results better than 10% with a standard lamp (Optronic Laboratories model 245C) the current must be regulated to better than 0.1%

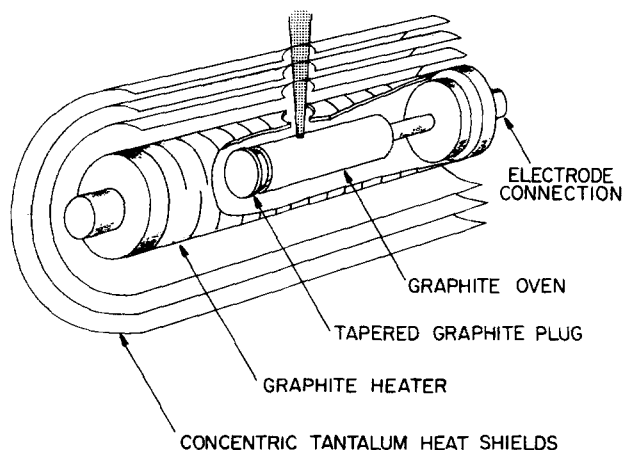


FIG. 2. Metal atom source, designed by R. C. Oldenborg.⁷ A few hundred amperes are passed through a graphite cylinder, held between two water-cooled copper bussbars. The graphite heater has slots cut on its body to increase the resistance. Inside the heater and supported from one end is a graphite crucible containing the metal sample.

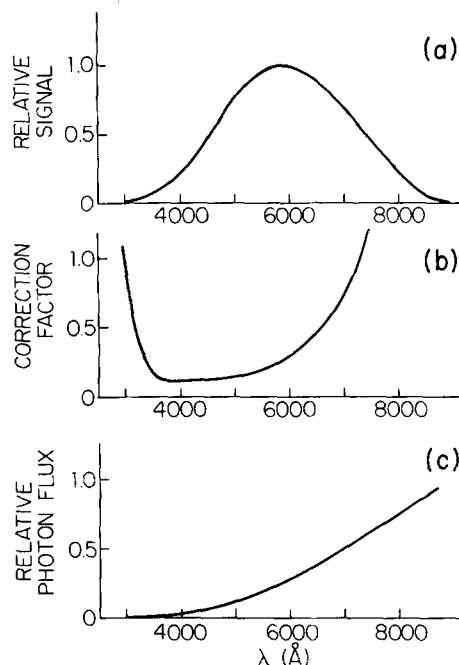


FIG. 3. (a) The spectrum of the standard lamp output,⁸ which is multiplied by the correction factor (b) to obtain (c) the relative photon flux of the standard lamp. In practice, (a) and (c) are known, while (b) is derived.

and the actual current measurement must be made better than 1%. The current may be measured by monitoring the voltage drop across a precision resistor with a digital voltmeter. Alternatively, the power supply (Optronic Laboratories model 65) may be used. Since this supply maintains the required 6.50 A to better than 0.1%, we have chosen the use of the power supply to ensure the best calibration. It is important that the lamp orientation and the polarity of the electrical connections to the lamp are made in the manner specified by the manufacturer if reproducible results are desired.

To obtain an absolute calibration of the spectra corrected on a relative basis a photomultiplier tube behind a slit of known area views the chemiluminescence through three different interference filters having a narrow bandwidth (< 30 Å). This optical-detection system (see Fig. 4) is calibrated on an absolute basis with the standard tungsten-iodine lamp. The calibrated output is listed in Table II for each interference filter. Thus, the need to

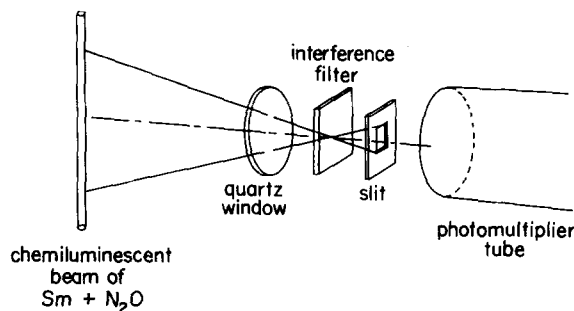


FIG. 4. Photon flux measurement apparatus. The distance from the beam to the slit is about 10.5 cm. The slit is a rectangular aperture, 0.3 cm high and 1.0 cm long.

TABLE II. Phototube and interference filter calibration.

$\lambda(\text{\AA})$	FWHM(\AA)	Phototube calibration ^a
6328.0	34	3.99×10^{14}
5262.5	17.5	8.39×10^{14}
4418.0	33	1.97×10^{14}

^aphotons $\text{sec}^{-1} \text{nm}^{-1} \text{cm}^{-2} \text{\AA}^{-1}$.

calibrate a spectrometer and lens arrangement on an absolute basis is entirely eliminated. While only one interference filter is necessary to provide an absolute calibration at all wavelengths, three such filters provide cross checks.

The Sm beam enters the scattering chamber through a 4.1 mm diameter hole, and the chemiluminescence appears as a very narrow, cylindrical beam of light. The geometry of the beam is not diffuse for the reaction of $\text{Sm} + \text{N}_2\text{O}$ because the radiative lifetime of SmO is 83 ± 2 nsec.⁹

Let the chemiluminescent emission per unit volume be denoted by E . Then the photon flux (F_D) at the detector is given by

$$F_D = A_D E V_{\text{obs}} / 4\pi r^2, \quad (1)$$

where A_D is the aperture area (0.3×1 cm) and V_{obs} is the volume of chemiluminescence defined by the detector field of view through the aperture. The volume of chemiluminescence (V_{obs}) actually observed was determined in two ways. A mask was gradually lowered into the field of view until a decrease in the chemiluminescent intensity was measured. From this observation we derive V_{obs} from a knowledge of the beam cross section. A second determination was made by surrounding the beam by a tube (~ 2 cm diam.) having its inside blackened. This tube had a 0.4×1 cm aperture which defined the reaction zone visible to the photomultiplier. The ratio of the chemiluminescent intensities without and with this additional slit should be the ratio V_{obs} to the known value of V_{obs} . The two V_{obs} determinations agreed within 8%. A more complete discussion is given in the Appendix.

To determine the number of photons emitted per second from this volume the chemiluminescent spectrum is corrected on a relative basis using the correction factors of Table I. The area under the chemiluminescent spectrum is proportional to the number of photons emitted per second. The absolute number of photons emitted per second is obtained by observing the chemiluminescence through an interference filter whose output is calibrated on an absolute basis (Table II). The total number of photons emitted per second in all directions is then found from Eq. (1). The spectrum range covered is 350–800 nm.

C. Metal flux

Because the "sticking coefficient" is not unity for most metals, quartz microbalance techniques and other thin film thickness monitors only measure the amount of

metal actually deposited on the sensor and *not* necessarily the true metal beam flux. Consequently, we chose to collect the metal beam using a thin, hollow, glass sphere having an entrance port slightly larger than the beam diameter (see Fig. 5). Since little metal can escape, we expect the results to be reliable. The amount of metal deposited over a given time period is then determined by weighing the collection vessel before and after deposition. In the case of barium the metal was allowed to convert completely to the oxide so that the best determination of the original amount of metal could be made. Five determinations were made of the Sm flux by collecting the metal over a 3 h period. The average weight was 0.0106 ± 0.0021 g. This corresponds to a Sm flux of 4.53×10^{15} atoms/cm² sec at the glass sphere 11 cm distant from the oven. Similarly, the barium flux was found to be 1.77×10^{16} atoms/cm² sec under the same conditions.

D. Oxidant flux

Pressure measurements are made with a corrosion-resistant capacitance manometer (Datametrics model 573A-10T-4A1-H5). Depending on the particular gas, the pressure read by an ionization gauge can be in error by a factor of 2 or 3 in the pressure range of 10^{-4} torr. Because of the reactivity of the various oxidant gases used, we found it impossible to calibrate an ion gauge against the capacitance manometer. The input port of the capacitance manometer (3/8 in. stainless steel tube approximately 6 in. long) was less than 1/4 in. away from the reaction zone viewed by the photomultiplier when the photon flux was being measured. Efforts were made to eliminate any adsorbed water this tube by heating it with a heat gun while the chamber was being evacuated. When the tube cooled sufficiently it could be accurately zeroed and remained reasonably stable over a few minutes before the zero would have to be readjusted slightly.

The reliability of capacitance manometer measurements has been checked by Loriot and Moran¹⁰ against the absolute pressure as measured by a McCleod gauge in the submillitorr pressure range. They find that the difference is $\sim 0.6\%$ over the pressure range 2×10^{-4} to 5×10^{-6} torr. Thus, we feel that the use of a capacitance manometer gives a trustworthy determination of the oxidant pressure.

E. Cross section measurements

At low pressures (10^{-5} to 10^{-4} torr) the chemiluminescence intensity obeys a $p \exp(-\alpha p)$ relationship, where p is the oxidant pressure.⁷ The linear term in p describes

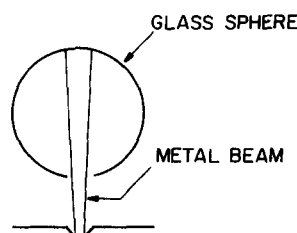


FIG. 5. Metal flux determination using a thin, hollow, glass sphere. In order to obtain a weighable sample the orifice of the entrance port to the scattering chamber is enlarged. While the number of metal atoms/sec that are collected increases, the flux (number of metal atoms/cm² sec) is not altered by the small change made.

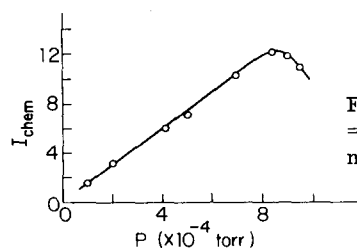


FIG. 6. Determination of $\sigma_{\text{tot}} = 82 \text{ \AA}^2$ from the pressure maximum for $\text{Sm} + \text{N}_2\text{O}$.

the formation of excited state molecules and the exponential term $\exp(-\alpha l)$ describes the attenuation of the metal beam by the oxidant. The attenuation parameter α in torr^{-1} is related to the total phenomenological cross section for metal atom removal σ_{tot} in \AA^2 by

$$\alpha = 1.33 \times 10^{-13} \frac{l \sigma_{\text{tot}}}{kT}, \quad (3)$$

where l is the beam path length (cm) in the reaction chamber from the port of entry to the reaction zone viewed by the spectrometer, k is the Boltzmann constant ($\text{erg}^\circ\text{K}^{-1} \text{molecule}^{-1}$), and T is the absolute temperature. The constant 1.33×10^{-13} has units of $\text{dyne torr}^{-1} \text{\AA}^{-2}$. The attenuation parameter can be determined in two independent ways:

(1) by studying the chemiluminescence intensity vs oxidant pressure for constant l ;

(2) by studying the chemiluminescence intensity vs l for a constant oxidant pressure.

The first method determines α from the pressure maximum

$$\alpha = 1/P_{\text{max}}, \quad (4)$$

from which σ_{tot} may be found using Eq. (3). A typical plot for the $\text{Sm} + \text{N}_2\text{O}$ reaction is given in Fig. 6. Although the chemiluminescent intensity appears linear with oxidant pressure for low pressures, the falloff is more rapid than expected. Consequently, the use of Eq. (4) to determine α is only a rough estimate. The second method plots $\ln I$ vs l (see Fig. 7); the slope of this plot is given by

$$\frac{d(\ln I)}{dl} = -1.33 \times 10^{-13} \left(\frac{P}{kT} \right) \sigma_{\text{tot}}, \quad (5)$$

from which σ_{tot} can be directly determined. The latter method is preferable since higher oxidant pressures are avoided.

TABLE III. Total phenomenological cross sections.

Reaction	$\sigma_{\text{tot}} (\text{\AA}^2)$	
	I_{chem} vs length ^a	I_{chem} vs pressure ^b
$\text{Sm} + \text{N}_2\text{O}$	89 ± 6	82
$\text{Sm} + \text{F}_2$	99 ± 8	95
$\text{Ba} + \text{NO}_2$...	122
$\text{Ba} + \text{N}_2\text{O}$	82 ± 6	92

^aSee Eq. (5).

^bSee Eq. (4).

TABLE IV. Absolute photon yields (%) as a function of pressure.^a

$P (10^{-4} \text{ torr})$	$\text{Sm} + \text{N}_2\text{O}$	$\text{Sm} + \text{F}_2$	$\text{Ba} + \text{N}_2\text{O}$	$\text{Ba} + \text{NO}_2$
0.6	0.32 ± 0.13
1.0	0.47 ± 0.15	...	2.25 ± 0.17	0.19
1.2	0.39 ± 0.15	0.18
1.5	...	11.8 ± 0.9
1.8	0.43 ± 0.17
2.0	0.60 ± 0.17	...	2.42 ± 0.58	...
2.1	0.17
3.0	...	10.9 ± 0.6	2.59 ± 0.39	...
3.2	...	12.8 ± 1.1
4.0	0.66 ± 0.09	...	2.33 ± 0.81	...
4.4	...	12.0 ± 0.9
5.0	0.90 ± 0.24	...	3.42 ± 0.90	...
6.0	2.91 ± 0.73	...
6.5	...	13.5 ± 0.6
6.7	0.20
7.0	3.70 ± 0.92	...
7.3	...	15.0 ± 0.9
7.5	3.62 ± 0.96	...
8.5	1.86 ± 0.79

^aErrors are one standard deviation (σ).

The total phenomenological cross sections for the $\text{Sm} + \text{N}_2\text{O}$, $\text{Sm} + \text{F}_2$, $\text{Ba} + \text{NO}_2$, and $\text{Ba} + \text{N}_2\text{O}$ reactions are given in Table III. Equation (5) is used except for $\text{Ba} + \text{NO}_2$, and the errors listed represent the maximum variation for five measurements at different pressures.

F. Photon yields

The chemiluminescence intensity (photons sec^{-1}) for the $\text{Sm} + \text{N}_2\text{O}$ reaction is given by

$$I_{\text{chem}} = k[\text{M}][\text{OX}]V_{\text{obs}} \quad (6)$$

under single-collision conditions, where V_{obs} is the observed reaction volume (cm^3), k is the rate constant ($\text{cm}^3 \text{sec}^{-1}$), and $[\text{M}]$ and $[\text{OX}]$ are concentrations (number per cm^3). The chemiluminescence cross section σ_{chem} is then determined from the relation

$$I_{\text{chem}} = \sigma_{\text{chem}} \bar{v}[\text{M}][\text{OX}]V_{\text{obs}}, \quad (7)$$

where \bar{v} is the average relative velocity of the metal atoms. Since the initial metal beam flux $[\text{M}_0]$ will be attenuated by a factor $e^{-\alpha l}$, this correction is included in estimating $[\text{M}]$ in the reaction zone. Thus, the chemiluminescence cross section is given by

$$\sigma_{\text{chem}} = \frac{I_{\text{chem}}}{(\bar{v}[\text{M}_0]e^{-\alpha l})([\text{OX}]V_{\text{obs}})}. \quad (8)$$

In Eq. (8) the first factor in the denominator is the metal

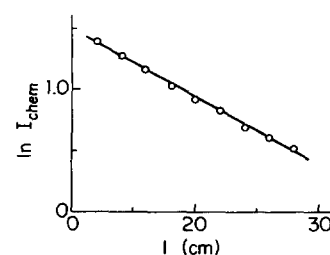


FIG. 7. Plot of the logarithm of the chemiluminescent intensity vs path length for the reaction $\text{Sm} + \text{N}_2\text{O}$. The data presented give a determination of $\sigma_{\text{tot}} = 91 \text{ \AA}^2$, which was included in the average reported in Table III.

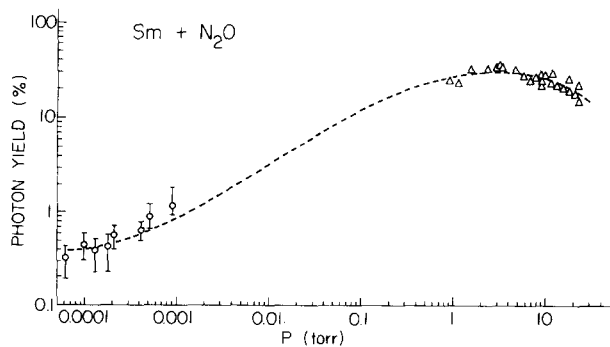


FIG. 8. Absolute photon yields as a function of pressure for the $\text{Sm} + \text{N}_2\text{O}$ reaction: (○) this work; and (△) Ref. 3. The dashed line is drawn to connect smoothly the low and high pressure data; no model is implied.

flux ($\text{atoms cm}^{-2} \text{sec}^{-1}$) in the reaction zone and the second factor is the number of oxidizer molecules in the reaction zone. With I_{chem} in units of photons sec^{-1} the dimensions of σ_{chem} are cm^2 . The photon yield in percent is taken to be the ratio of the chemiluminescence cross section to the total cross section

$$\Phi = \frac{\sigma_{\text{chem}}}{\sigma_{\text{tot}}} \times 100 \quad (9)$$

Since σ_{tot} includes wide-angle nonreactive scattering processes (e.g., inelastic collisions), Φ is actually a lower bound. However, when the reactive cross section is large, such as in these cases, σ_{tot} is expected to be a good approximation to the total reactive cross section.

III. RESULTS

The photon yields for the reactions $\text{Sm} + \text{N}_2\text{O}$, $\text{Sm} + \text{F}_2$, $\text{Ba} + \text{N}_2\text{O}$, and $\text{Ba} + \text{NO}_2$ were determined at various pressures. Often several measurements were made at each pressure and the results, given in Table IV, represent average values. Figures 8–12 show the actual spread in the data for each of the above reactions. The dotted lines connect the absolute photon yields obtained at pressures of several torr argon to the average values in the submillitorr region.

Palmer and co-workers^{5,11} have measured photon yields in the 0.01–0.1 torr pressure regime for the $\text{Ba} + \text{N}_2\text{O}$ and $\text{Ba} + \text{NO}_2$ reactions. Our measurements provide a low pressure intercept that connects to their data

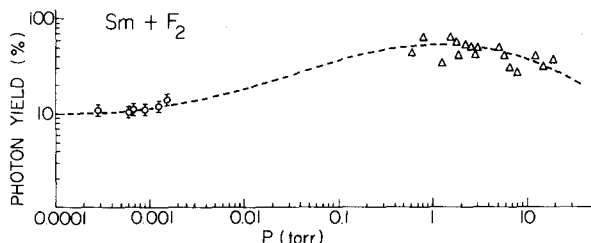


FIG. 9. Absolute photon yields as a function of pressure for the $\text{Sm} + \text{F}_2$ reaction: (○) this work; and (△) Ref. 3. The dashed line is drawn to connect smoothly the low and high pressure data; no model is implied.

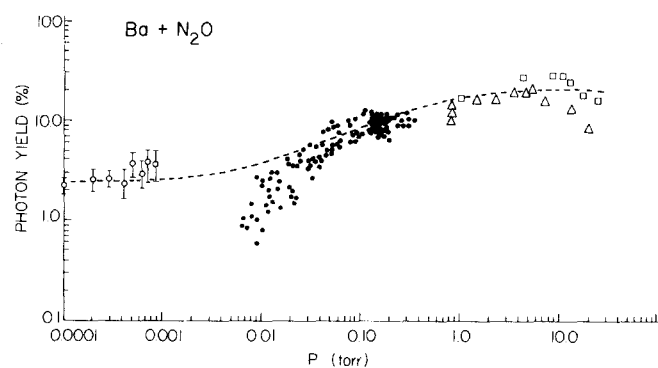


FIG. 10. Absolute photon yields as a function of pressure for the $\text{Ba} + \text{N}_2\text{O}$ reaction: (○) this work; (●) Ref. 11; (△) Ref. 3; and (□) Ref. 6. The dashed line is drawn to connect smoothly the low and high pressure data; no model is implied.

very well. While no measurements exist in the 0.01–0.1 torr pressure range for the $\text{Sm} + \text{N}_2\text{O}$ and $\text{Sm} + \text{F}_2$ reactions, the dotted line should predict the photon yields where they have not been measured. The intercepts provide data that may help to model the high-pressure reaction kinetics for these systems.

The estimated uncertainties in the absolute photon yields are $\sim 50\%$, where the estimated uncertainty for σ_{tot} is $\sim 10\%$, I_{chem} is 10% , $[\text{M}]$ is $\sim 20\%$, and $[\text{OX}]$ is $\sim 10\%$. The most serious error is associated with the metal flux determinations. For the reaction $\text{Sm} + \text{N}_2\text{O}$ at a pressure of 8.5×10^{-4} torr the photon yield was measured 10 times giving $\Phi = 1.86 \pm 0.79$, where the error represents one standard deviation. This error is a 43% uncertainty, but some standard deviations for the $\text{Sm} + \text{N}_2\text{O}$ and $\text{Ba} + \text{N}_2\text{O}$ reactions at other pressures were 10%–20% of the average value. The 50% uncertainty represents an estimate of all errors, statistical and systematic. As can be seen from Table IV the scatter of the measurements is much smaller.

We previously reported a preliminary photon yield of 0.3% for the reaction $\text{Sm} + \text{N}_2\text{O}$ at a pressure of 4×10^{-4} torr.¹² The value at this same pressure given in Table IV is 0.66%. However, the preliminary value did provide a reasonable order of magnitude estimate.

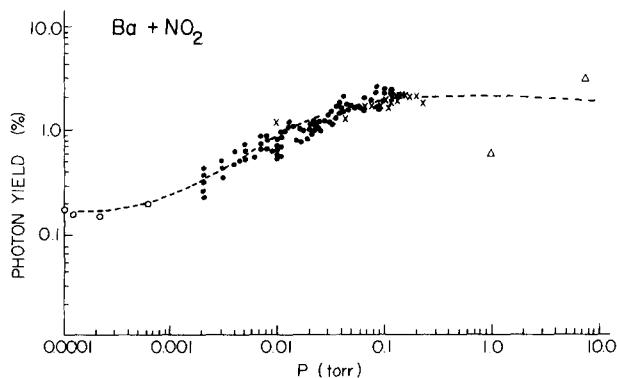


FIG. 11. Absolute photon yields as a function of pressure for the $\text{Ba} + \text{NO}_2$ reaction: (○) this work; (●) and (×) Ref. 11; and (△) Ref. 6. The dashed line is drawn to connect smoothly the low and high pressure data; no model is implied.

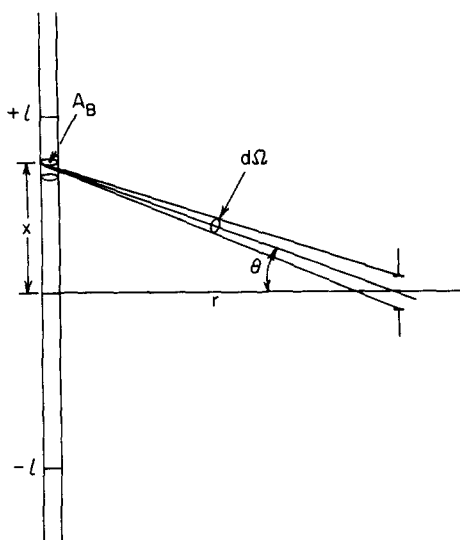


FIG. 12. Geometry for describing the measurement of flux from a finite cylindrical light source.

Yokozeiki and Menzinger¹³ recently measured *relative* photon yields for several Sm and Yb reactions in the 5×10^{-6} – 5×10^{-8} torr range, also using a beam-gas arrangement. They found at $\leq 1 \times 10^{-4}$ torr that the ratio of the photon yield for the Sm + N₂O reaction to that of the Sm + F₂ reaction is 0.13. This should be compared with our photon yield ratio of 0.036. The large discrepancy arises from the difference between the total reactive cross sections used in these two studies. Because we have two independent measurements on σ_{tot} , we believe our values are to be preferred. A similar disagreement occurs for the reaction of Ba + N₂O under beam conditions. Menzinger¹⁴ finds a total phenomenological cross section of about 30 Å². While this agrees with previous work,⁷ it disagrees with the present value of 82 Å².

One remarkable result of this study is that the absolute photon yield for the Sm + F₂ reaction is ~12% under single-collision conditions. Our previous estimate was only ~1% because of errors associated with the measurements of the F₂ pressure and the determination of V_{obs} . The high photon yield for the Sm + F₂ reaction is very interesting because it suggests that there may be other chemical reactions with an appreciable probability for producing electronically excited products in the initial reaction step.

ACKNOWLEDGMENTS

We thank D. J. Eckstrom for critically reading an earlier draft of this paper and for helping us to calculate the photon flux. We are also grateful to H. B. Palmer and M. Menzinger for providing us with unpublished data. This research was supported by the Advanced Research Projects Agency of the Department of Defense, monitored by the Office of Naval Research under contract N00014-76-C-0466, and by the Air Force Office of Scientific Research under contract AFOSR-73-2551.

APPENDIX: PHOTON FLUX FROM A CYLINDRICAL CHEMILUMINESCENT BEAM

The following considerations are due to D. J. Eckstrom, who provided us with the calculations of the photon flux

from a cylindrical light source of variable extent: The chemiluminescent beam is assumed to have a cross section A_B of uniform emission. The aperture through which the emission is viewed is at a distance r and has an area A_D . The detector is capable of viewing the chemiluminescence over a distance $+l$ to $-l$ as shown in Fig. 12. If the emission per unit volume is

$$E(x) = \sigma_{\text{chem}} \bar{v} [M_0 e^{-\sigma_{\text{tot}} N x}] [\text{OX}] , \quad (\text{A1})$$

where N is the number of oxidant molecules per unit volume, then the photon flux at the detector is

$$F_D = \int_{-l}^{+l} dx A_B E(x) \frac{d\Omega}{4\pi} , \quad (\text{A2})$$

where

$$d\Omega = \frac{A_D \cos\theta}{x^2 + r^2} = \frac{r A_D}{(x^2 + r^2)^{3/2}} . \quad (\text{A3})$$

Thus,

$$F_D = A_B A_D \frac{r}{4\pi} \int_{-l}^{+l} \frac{E(x) dx}{(x^2 + r^2)^{3/2}} . \quad (\text{A4})$$

When $E(x) = E = \text{constant}$, then

$$F_D = A_B A_D \frac{E r}{4\pi} \frac{2l}{r^2 \sqrt{l^2 + r^2}} . \quad (\text{A5})$$

For $l \gg r$, i. e., an infinite beam, Eq. (A5) becomes

$$F_D = \frac{A_B A_D E}{2\pi r} . \quad (\text{A6})$$

Here the light flux only falls off by the reciprocal of the distance.

For $l \ll r$, i. e., a small source, Eq. (A5) becomes

$$F_D = A_D E \frac{A_B 2l}{4\pi r^2} = V_{\text{obs}} E \frac{A_D}{4\pi r^2} \quad (\text{A7})$$

and the light flux falls off by the reciprocal of the square of the distance.

For $l \sim r$, i. e., a beam of finite length, Eq. (A5) becomes

$$F_D = A_B 2l E \frac{A_D}{4\pi r \sqrt{l^2 + r^2}} = V_{\text{obs}} E \frac{A_D}{4\pi r \sqrt{r^2 + l^2}} . \quad (\text{A8})$$

Since $(l^2 + r^2)^{1/2} \simeq r$ in this case, Eq. (A8) is approximated by Eq. (A7), i. e., the falloff is as r^{-2} .

Suppose, however, that E decreases exponentially, as in the case of the beam-gas chemiluminescence, i. e.,

$$E(x) = E_0 \exp(-\sigma_{\text{tot}} N x) . \quad (\text{A9})$$

Then,

$$F_D = \int_{-l}^{+l} dx A_B E_0 \exp(-\sigma_{\text{tot}} N x) \frac{d\Omega}{4\pi} \quad (\text{A10})$$

$$\simeq A_B E_0 \frac{d\Omega}{4\pi} \frac{1}{\sigma_{\text{tot}} N} [\exp(\sigma_{\text{tot}} N l) - \exp(-\sigma_{\text{tot}} N l)] . \quad (\text{A11})$$

Since $\sigma_{\text{tot}} N l$ is small, Eq. (A11) becomes

$$F_D = A_B 2l E_0 \frac{A_D}{4\pi r^2} . \quad (\text{A12})$$

Comparing Eq. (A12) with (A7) we conclude that for small $\sigma_{\text{tot}} N l$ they are identical and the exponential decay of the

beam introduces no additional correction to the flux measurement.

- ¹D. J. Eckstrom, S. A. Edelstein, and S. W. Benson, *J. Chem. Phys.* **60**, 2930 (1974).
- ²G. Black, M. Luria, D. J. Eckstrom, S. A. Edelstein, and S. W. Benson, *J. Chem. Phys.* **61**, 4932 (1974).
- ³D. J. Eckstrom, S. A. Edelstein, D. L. Huestis, B. E. Perry, and S. W. Benson, *J. Chem. Phys.* **63**, 3828 (1975).
- ⁴R. H. Obenauf, C. J. Hsu, and H. B. Palmer, *J. Chem. Phys.* **57**, 5607 (1972); **58**, 2674E (1973); **58**, 4693 (1973).
- ⁵C. J. Hsu, W. D. Krugh, and H. B. Palmer, *J. Chem. Phys.* **60**, 5118 (1974).
- ⁶C. R. Jones and H. P. Broida, *J. Chem. Phys.* **59**, 6677 (1973); **60**, 4369 (1974).
- ⁷Ch. Ottinger and R. N. Zare, *Chem. Phys. Lett.* **5**, 243 (1970); C. D. Jonah, R. N. Zare, and Ch. Ottinger, *J. Chem. Phys.* **56**, 263 (1972); J. L. Gole and R. N. Zare, *J. Chem. Phys.* **57**, 5331 (1972); R. C. Oldenborg, J. L. Gole, and R. N. Zare, *J. Chem. Phys.* **60**, 4032 (1974); R. C. Oldenborg, Ph.D. Thesis, Columbia University (1975).
- ⁸R. Stair, W. E. Schneider, and J. K. Jackson, *Appl. Opt.* **2**, 1151 (1963). The standard lamp supplied by Optronics Laboratories is certified by W. E. Schneider.
- ⁹C. R. Dickson, Ph.D. Thesis, Columbia University (1976).
- ¹⁰G. Loriot and T. Moran, *Rev. Sci. Instrum.* **46**, 140 (1975).
- ¹¹H. B. Palmer (private communication, preliminary results, July, 1976).
- ¹²C. R. Dickson and R. N. Zare, *Chem. Phys.* **7**, 361 (1975).
- ¹³A. Yokozeki and M. Menzinger, *Chem. Phys.* **14**, 427 (1976).
- ¹⁴M. Menzinger (private communication).